ELASTIC WAVE PROPAGATION IN ANISOTROPIC MEDIA

Thesis for the Degree of M. S.

MICHIGAN STATE UNIVERSITY

JUERGEN H. STAUDTE

1967

ELASTIC WAVE PROPAGATION IN ANISOTROPIC MEDIA

By

Juergen H. Staudte

AN ABSTRACT OF A THESIS

ABSTRACT

ELASTIC WAVE PROPAGATION IN ANISOTROPIC MEDIA

by

Juergen H. Staudte

The propagation of plane elastic waves in an aniso-
tropic material is investigated. Using a compact tensor nota-
tion, the theory is developed such that the fundamental quantities
necessary to describe wave propagation can be calculated. These
include the velocities of the wavefronts of the acoustic beam,
the particle displacement vectors, and the directions of the
energy flow. A computer program, which numerically calculates
these quantities, is included.

As the wave propagation properties of light are similar
and in general, are better known, the optical theory is reviewed,
using Maxwell's equations as a basis. Light propagation is
studied by using such concepts as wave surfaces and normal velocity
surfaces; the same surfaces are generated for elastic waves from
the numerical results of the computer program. From this, the
anomaly of cuspidal edges on the wave surfaces of elastic waves
is discussed.

The similarities between conical refraction for light
and elastic waves are discussed. The pertinent quantities
associated with elastic conical refraction are calculated for
quartz.

ELASTIC WAVE PROPAGATION IN ANISOTROPIC MEDIA

By

Juergen H. Staudte

A THESIS

Submitted to
Michigan State University
in partial fulfillment of the requirements
for the degree of

MASTER OF SCIENCE

Department of Physics

1967

ACKNOWLEDGEMENT

ii

TABLE OF CONTENTS

LIST OF FIGURES

A vector $\bar{D}$ linearly related to a vector $\bar{E}$ in the manner

$$\begin{vmatrix} D_1 \\ D_2 \\ D_3 \end{vmatrix} = \begin{vmatrix} \epsilon_{11} & \epsilon_{12} & \epsilon_{13} \\ \epsilon_{21} & \epsilon_{22} & \epsilon_{23} \\ \epsilon_{31} & \epsilon_{32} & \epsilon_{33} \end{vmatrix} \begin{vmatrix} E_1 \\ E_2 \\ E_3 \end{vmatrix}$$

where 1, 2 and 3 represent x, y and z respectively, can be written in the simpler form

$$D_i = \sum_{j=1}^{3} \epsilon_{ij} E_j \, .$$

Further simplification can be achieved by introducing the Einstein summation convention: when a small letter subscript occurs twice in the same term, summation with respect to that subscript is to be automatically understood. The above equation can, therefore, be written as

$$D_i = \epsilon_{ij} E_j \, .$$

A quadratic term such as U_i^2 will mean $U_i \cdot U_i$ and, therefore, summation will be understood. The subscripts i, j, k and l will represent the coordinate components. The capital letter N used as a subscript will only be a label for the N'th root and, therefore, is excluded from the usual rules of tensor summation. All summation will be understood to be from 1 to 3.

Any vector quantity such as $\bar{E}$ can have auxiliary quantities defined as follows:

a) E the magnitude of $|\bar{E}|$;

b) $\hat{E}$ the unit vector in the direction of $\bar{E}$;

c) E_i the i'th component of the vector $\bar{E}$.

$\bullet$	Dot above a letter denotes differentiation with respect to time.
$\hat{e}$	Unit vector along the i'th coordinate axis
x_i	Spatial coordinate: $x_1 = x$; $x_2 = y$; $x_3 = z$.
$\bar{r}$	$x_i \hat{e}_i$
∇	$\dfrac{\partial}{\partial x_i} \hat{e}_i$
$\bar{A}$	Amplitude vector
a_{Ni}	The i'th direction cosine of the N'th elastic displacement eigenvector
$\bar{B}$	Magnetic flux density vector
c	Speed of light in a vacuum
c_{ijkl}	Elastic constants (rank four tensor)
d_{Ni}	The i'th direction cosine of the N'th electric displacement eigenvector
$\bar{D}$	Electric displacement
$\bar{E}$	Electric field vector
$\bar{H}$	Magnetic field intensity vector
$\bar{K}$	Plane wave propagation vector
$\bar{l}$	$l_i \hat{e}_i$ where l_i are the direction cosines denoting the direction of
$\bar{N}_N$	The N'th normal velocity vector
$\hat{P}$	Elastic Poynting vector
$\bar{R}_N$	The N'th ray vector
S	Electric Poynting vector
t	Time
$\bar{U}$	Particle displacement vector

vi

υ Phase velocity of plane wave

V_i Defined as $1/\epsilon_i \mu_0$

W Potential energy per unit volume

δ_{ij} Kroenecker delta ; $\delta_{ij} = \begin{array}{l} 0 \text{ if } i \neq j \\ 1 \text{ if } i = j \end{array}$

ϵ_{ij} Permittivity or strain tensor

ϵ_i Components of diagonalized   - tensor

μ_0 Permiability in a vacuum

σ_{ij} Stress tensor

ω Angular frequency

CHAPTER I

INTRODUCTION

The study of light and elastic wave propagation have a
common history in their early development. With the publication
of Huygens' treatise[1] in 1690, the study of wave propagation began.
Since light was thought to be propagated through the aether, which
was conceived to be an elastic solid, the elastic theory was devel-
oped to a great extent. Not until 1817 was the transverse nature
of light suggested by Young and, ten years later, incorporated
into the theory of crystal optics by Fresnel[2]. From this point
on, the longitudinal nature of wave propagation was neglected
for some time. Christoffel[3] in 1877 wrote a memoir on elastic
wave propagation in anisotropic media and developed a method for
calculating phase velocities for three plane waves originating
from an arbitrary disturbance in a plane. The technique for the
determination of the characteristic displacement vectors associated
with these plane waves was given by Lord Kelvin in his Baltimore
Lectures[4] in 1904. In 1927, Love[5] developed an expression to cal-
culate the direction of the energy flow for each of the plane waves.

Wave behavior in crystals is usually analyzed by studying
the propagation of a disturbance which originated at a point, or
which is a plane wave. Both concepts are useful and correct, and
they can be derived from each other. Huygens' principle considers
only point sources; plane waves can be constructed from an infinite
set of point sources. When the plane wave approach is used, the

1

point source can be constructed from an infinite set of plane

waves that travel in all directions. The surface of equal phase

of a disturbance that is generated by a point source is called

the wave surface. By using Huygens' construction, the direction

and velocity of energy flow for $\overset{Q}{\underset{\wedge}{}}$ plane source can be determined.

When a disturbance is a plane wave, the velocity normal to the

plane of equal disturbance is called the normal velocity or the

phase velocity of the plane wave. In practice, the point source

approach is most useful in graphical techniques, and for con-

structing models for better comprehension of the problem; but

for analytical work, the plane wave techniques are more suitable

because more powerful mathematical methods are available.

The disturbances can be of quite different nature.

Only two will be discussed in this paper, namely the electromag-

netic wave in the form of light, and the focus of our discussion,

the elastic wave. Light is studied in Chapter II for comparison

and for the better understanding of the wave surfaces and wave

vectors or elastic waves.

Many different approaches for solving elastic wave

propagation problems have been introduced over the years. Usually

the different methods did not introduce anything new but they

rather presented the methods of Kelvin and Love in a simpler form

by taking special conditions into consideration. This paper will

discuss in detail the earlier mentioned developments in tensor

notation. The results of an experiment which renders visible

elastic waves are used to illustrate the main features of elastic propagation in anistropic media.

From some numerical results calculated using the computer program in Appendix C, several propagation phenomena of elastic waves are discussed. These include the existence of bicuspidal edges on wave surfaces. The appearance of bicuspidal edges imply that as many as five distinct signals from a point source may be observed. The possibility of this type of surface was first dis-covered by Musgrave[6] about ten years ago. Surfaces calculated using the theory presented here are the same as those calculated by Musgrave[6-8] using a different technique.

Conical refraction in optics is discussed and the basic principles are extended to elastic waves. A numerical example is presented for quartz. Also, a graphical method for presenting energy flow and characteristic particle displacement is suggested and demonstrated.

CHAPTER II

THE THEORY OF THE PROPAGATION OF LIGHT
IN ANISOTROPIC MEDIA

The fundamental properties of light propagation in crystals can be derived from Maxwell's equations. For an infinite, homogenous, nondissipative material with no sources present, Maxwell's equations can be written as follows:

$$\nabla \times \bar{E} = -\frac{1}{c}\dot{\bar{B}} \; ; \tag{1}$$

$$\nabla \times \bar{H} = \frac{1}{c}\dot{\bar{D}} \; ; \tag{2}$$

and

$$\nabla \cdot \bar{D} = \nabla \cdot \bar{B} = 0 \; . \tag{3}$$

The interaction of the electric field $\bar{E}$ with nonferrous materials is of the order of 10^5 larger than the interaction of the magnetic field intensity $\bar{H}$. For this reason, only interactions of the electric field with the material are considered. The electric displacement $\bar{D}$ is linearly related to $\bar{E}$ by the dielectric or permittivity tensor in the following manner:

$$D_i = \epsilon_{ij} E_j \; . \tag{4}$$

For convenience, we let the axes of the chosen coordinate system coincide with the principal axes of the ϵ_{ij} quadric, and then we can write

$$D_i = \epsilon_i E_i \; , \tag{5}$$

4

etc. The wave equation for an electromagnetic wave can now be constructed by substituting Eq. 2 into the curl of Eq. 1 which gives

$$\nabla \times \nabla \times \bar{E} = -\frac{\mu_0}{c^2}\ddot{\bar{D}} = \nabla(\nabla \cdot \bar{E}) - \nabla^2\bar{E}, \qquad (6)$$

where μ_0 is the permeability $(\bar{B} = \mu_0\bar{H})$ and c is the speed of light in a vacuum. A plane wave solution of Eq. 6 will be assumed; i.e.,

$$\bar{E} = \bar{\mathcal{E}}\exp[i(\bar{K}\cdot\bar{r} - \omega t)]. \qquad (7)$$

$\bar{K}$ is the propagation vector whose components can be written as $K_i = K\ell_i$ where ℓ_i are direction cosines. It is also noted that the phase velocity υ of the plane wave is $\frac{\omega}{K}$. Equation 7 can, therefore, be rewritten as

$$\bar{E} = \mathcal{E}_i\hat{e}_i\exp[iK(\ell_j x_j - \upsilon t)], \qquad (8)$$

where $\hat{e}_i$ is the coordinate unit vector. Substituting Eq. 8 into Eq. 6, we get

$$\frac{\mu_0}{c^2}K^2\upsilon^2 D_i - K^2\ell_i(\bar{\ell}\cdot\bar{E}) - K^2|\bar{\ell}\cdot\bar{\ell}|E_i = 0. \qquad (9)$$

Simplifying and rewriting Eq. 9 in component form and noting that $\bar{\ell}\cdot\bar{\ell} = 1$, we obtain for one component

$$\frac{\mu_0}{c^2}\upsilon^2 D_1 - \frac{D_1}{\mathcal{E}_1} + \ell_1(\bar{\ell}\cdot\bar{E}), \qquad (10)$$

or

$$D_1 = \frac{\ell_1 (\bar{\lambda} \cdot \bar{E})}{1/\epsilon_1 - \mu_0 v^2} ,$$

(11)

and similar expressions for the other components. If we calculate $\nabla \cdot \bar{D} = 0$, we find

$$\frac{\ell_i^2 (\bar{\lambda} \cdot \bar{E})}{1/\epsilon_i - \mu_0 v^2} = 0 ,$$

(12)

or on multiplying by $\mu_0 / \bar{\lambda} \cdot \bar{E}$,

$$\frac{\ell_i^2}{1/\epsilon_i \mu_0 - v^2} = 0 .$$

(13)

Let us define $V_i = 1/\epsilon_i \mu_0$. Equation 11 and Eq. 12 can now be rewritten as

$$D_1 = \frac{\bar{E} \cdot \bar{\lambda}}{\mu_0} \cdot \frac{\ell_1}{V_1^2 - v^2}$$

(14)

and

$$\frac{\ell_i^2}{V_i^2 - v^2} = 0$$

(15)

Written out and simplified, Eq. 15 becomes

$$\ell_1^2 (V_2^2 - v^2)(V_3^2 - v^2) + \ell_2^2 (V_1^2 - v^2)(V_3^2 - v^2) + \ell_3^2 (V_1^2 - v^2)(V_2^2 - v^2) = 0.$$

(16)

Equation 16 is a quadratic equation in v^2 and therefore has two roots which will be written as v_N^2 where $N = 1, 2$. A capital letter N used as a subscript will only be a label for

the N'th root and, therefore, is excluded from the usual rules of tensor summation. These two velocities υ_N, known as the characteristic or eigenvelocities, are associated with two directions or eigenvectors into which an arbitrary electric displacement is resolved. These eigenvectors can be calculated by substituting υ_N^2 into Eq. 14, which yields the components of the displacement vectors. The direction cosines d_{Ni} of the eigenvectors are now obtained from the normalized ratios of these components

$$d_{Ni} = \frac{\gamma_{Ni}}{\sqrt{\gamma_{Nj}^2}} \; ,$$

where

$$\gamma_{N1} = \frac{D_{N1}}{D_{N1}} = 1 \; ;$$

and

$$\gamma_{N2} = \frac{D_{N2}}{D_{N1}} = \frac{\ell_2 (V_1^2 - \upsilon_N^2)}{\ell_1 (V_2^2 - \upsilon_N^2)} \; ;$$

$$\gamma_{N3} = \frac{D_{N3}}{D_{N1}} = \frac{\ell_3 (V_1^2 - \upsilon_N^2)}{\ell_1 (V_3^2 - \upsilon_N^2)} \; .$$

(17)

It can be shown that the two displacement eigenvectors are orthogonal by using Eq. 16 to prove that their scalar product is zero.

With the information obtained up to this point, we can find the power flow using Poynting's theorem. The power flows along a vector $\bar{S}$, known as the Poynting vector, where

$$\bar{S} = \frac{c}{4\pi} (\bar{E} \times \bar{H}) \; .$$

(18)

We are not interested in the magnitude of the power flow but just the direction. The electric vector, which is necessary to calculate $\bar{S}$ in Eq. 18, can be obtained from the electric displacement eigenvector by using Eq. 5. Two electric vectors $\bar{E}_N$ are found and, therefore, two different $\bar{S}_N$ will result. From Maxwell's equations, we know that $\bar{D}$ is perpendicular to $\bar{K}$, and both $\bar{E}$ and $\bar{D}$ are perpendicular to $\bar{H}$. Equation 18 shows $\bar{S}$ to be perpendicular to $\bar{E}$ and $\bar{H}$ and, therefore, $\bar{D}$, $\bar{E}$, $\bar{K}$, and $\bar{S}$ are in the same plane (see Fig. 1). Figure 2 shows a three dimensional picture of a beam of light of arbitrary displacement
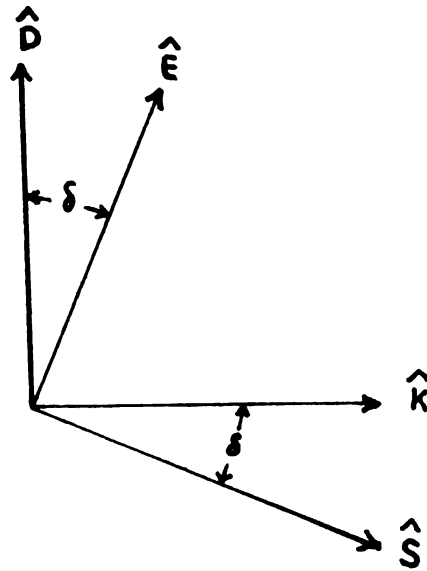
Figure 1. Diagram showing the relationship of vectors of an electromagnetic wave. For a plane wave with displacement $\bar{D}$ and electric field $\bar{E}$, the energy will flow along $\bar{S}$ and the wavefronts are normal to $\bar{K}$. All vectors shown are in the plane of the paper. The magnetic field $\bar{H}$ (not shown) points perpendicularly out of the paper.
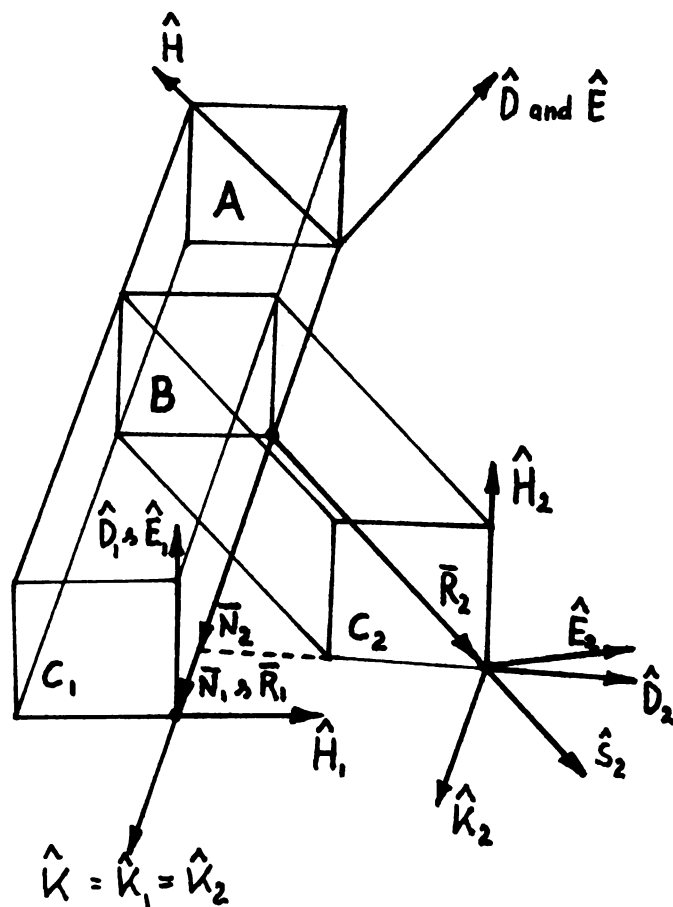
Figure 2. **Diagram showing the propagation**
characteristics of an electromagnetic
wave in an anisotropic medium. The
incoming light of arbitrary polarization
$\vec{D}$ upon entering the medium at B is re-
solved into two beams of discrete polar-
ization $\vec{D}_1$ and $\vec{D}_2$. The wave fronts
A, B, C_1 and C_2 are parallel and denote
the successive positions after increments
of unit time. The normal velocity vectors
$\vec{N}_1$, $\vec{N}_2$ show the magnitude of the vel-
ocity in the direction of the ray vectors
$\vec{R}_1$, $\vec{R}_2$ indicate the ray velocities in the
directions of the power flows.

entering an anisotropic solid at normal incidence to the surface.
Illustrated in the figure are all previously discussed vectors
for the case where the beam is split into two beams: one where
$\overline{D}$ is parallel to $\overline{E}$, and the other where it is not.

   If $\overline{K}$ is varied and the subsequent end points of $\overline{R}_1$
and $\overline{R}_2$ (as defined in Fig. 2) are plotted, the envelope of these
points will produce two surfaces which are the wave surfaces.
Using the same procedure for $\widetilde{N}_1$ and $\widetilde{N}_2$, two other surfaces
are produced which are the normal velocity surfaces. From
Fig. 2, we can see that $\overline{N}_1$ and $\widetilde{N}_2$ are perpendicular to their
respective wavefronts. The end points of $\overline{R}_1$ and $\overline{R}_2$ (which
originate in the plane B) lie in the planes of their respective
wavefronts. Each wavefront will be shown later to be tangent to
a wave surface at some point. Figure 3 illustrates in two dimen-
sions the construction of both surfaces by the method described
above. The locus of endpoints of the vectors $\overline{R}$ and $\overline{N}$ define
the wave surface and normal velocity surface, respectively. For
a particular $\overline{R}$ and $\widetilde{N}$, the line connecting the endpoints of
the two vectors will lie in the plane of the wavefront. The
construction and the relationship of the two types of surfaces
to each other can be seen in Fig. 3. Having constructed the
wave surfaces, the phase velocity and the ray direction can be
obtained graphically from Fig. 4. For a plane wave of direction
$\overline{ON}$ (see Fig. 4), the wavefront or line $\overline{RN}$ must be constructed
in such a way as to be perpendicular to $\overline{ON}$ and tangent to a point
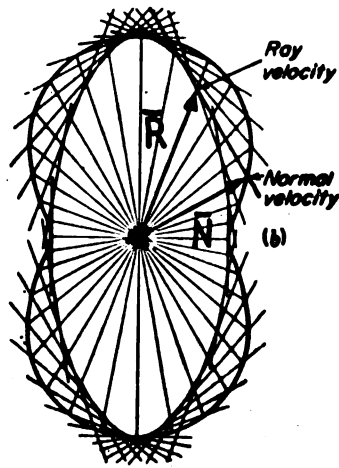
Figure 3. The wave surface (inner) and normal velocity surface (outer) as defined by the ray vector and normal velocity vector.
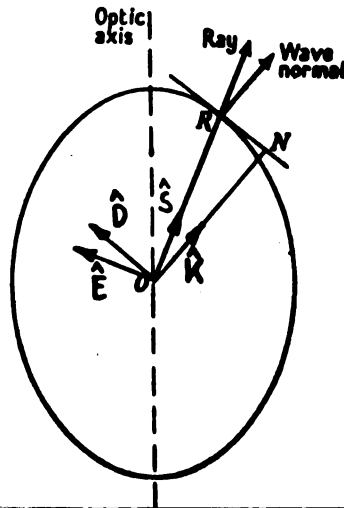
Figure 4. Construction of the wave surface from the normal velocity and ray velocity.
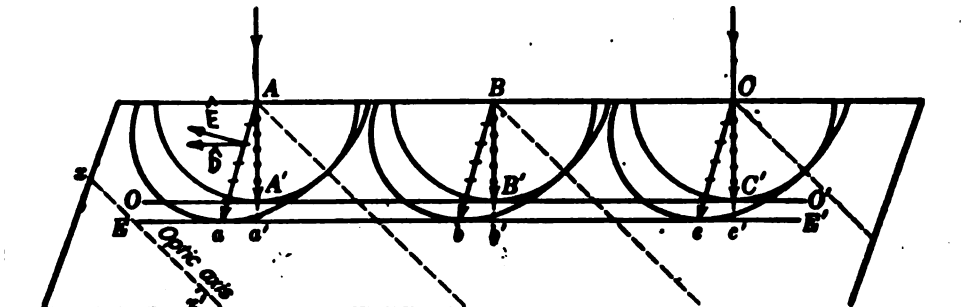
Figure 5. Construction of the envelopes defining plane waves from point sources using Huygens' principle.

on the wave surface which occurs at the only possible point of
contact. This point of contact R will give us the direction
of the ray $\overline{OR}$. The ray velocity is defined by the length OR ;
the normal velocity $\mathcal{V}_N$ is given by ON. The polarization or
electric displacement can be recovered by considering Fig. 1.
The points R , O , and N define the plane in which the vectors
$\overline{D}$, $\overline{E}$, $\overline{K}$, and $\mathcal{S}$ lie. Therefore, we illustrate in Fig. 4
a simple construction that yields $\overline{D}$ and $\overline{E}$. As two surfaces
exist for electromagnetic waves, the previous considerations will
hold for both, and therefore enable us to obtain the quantities
for both resolved rays.

If a point source of light were placed in a material,
generally two sets of wavefronts would emanate from this point;
each set having the shape of one of the wave surfaces. This is
true, since such a point source may be considered to be composed
of an infinite set of plane waves. Conversely, a plane source
can be thought of as an infinite set of point sources which radiate
coherently. The electric displacements of wave surfaces from each
of the point sources will interfere and will only have nonvanish-
ing amplitude in the envelope of all the wave surfaces. This
construction is known as Huygens' construction and is illustrated
in fig. 5.

It shall be noted that quantitatively the use of the
wave surfaces has many limitations. The graphical method which
must be applied produces only approximate numerical results.

Moreover, these representations are limited to two dimensions. Nevertheless, they are very useful in explaining propagation phenomena qualitatively, in predicting anomalies, and in showing the overall picture. Their usefulness will become obvious when conical refraction is studied in a later chapter.

In the next chapter the same approach as used in this chapter will be taken for obtaining some insight into the behavior of elastic waves; also, we will draw heavily on the results of this chapter.

CHAPTER III

THE THEORY OF THE PROPAGATION OF ELASTIC WAVES

IN ANISOTROPIC MEDIA

In order to study the behavior of elastic waves, we must determine essentially the same vectors, surfaces and velocities as in the case of light. Again, we will construct the wave equation and the solution will be assumed to be a plane wave. We will let the stresses, strains and particle displacements be linearly related to each other and nonlinear effects, which are small, will be neglected.

For a linear anisotropic material the following tensor relationship expresses Hooke's law:

$$\sigma_{ij} = C_{ijkl}\, \epsilon_{kl} \tag{19}$$

where σ_{ij} are the components of stress tensor, ϵ_{kl}, the strain tensor and C_{ijkl} are known as the elastic constants. The components of strain are related to the particle displacement $\overline{U}$ by

$$\epsilon_{kl} = \frac{1}{2}\left(\frac{\partial U_k}{\partial x_l} + \frac{\partial U_l}{\partial x_k} \right). \tag{20}$$

Newton's second law for a continuous medium can be written as

$$F_j = \rho_0\, \ddot{U}_j \tag{21}$$

where ρ_0 is the equilibrium density of the medium. This force F_j arises from stress gradients in the material,

14

$$F_j = \frac{\partial \sigma_{ij}}{\partial x_i} . \tag{22}$$

Combining Eq. 21 and Eq. 22, we get the following equation for a linear homogenous, continuous, anisotropic medium,

$$\rho_0 \ddot{U}_j = \frac{\partial \sigma_{ij}}{\partial x_i} . \tag{23}$$

Substituting Eq. 19 and Eq. 20 into Eq. 23, we obtain the wave equation:

$$\rho_0 \ddot{U}_j = \frac{1}{2} C_{ijkl} \frac{\partial}{\partial x_i} \left(\frac{\partial U_k}{\partial x_l} + \frac{\partial U_l}{\partial x_k} \right) . \tag{24}$$

For the above differential equation we will assume a plane wave solution given by

$$\bar{U} = \bar{A} \exp\left[i \left(\bar{K} \cdot \bar{r} - \omega t \right) \right] . \tag{25}$$

The phase velocity of a plane wave is given by $v = \frac{\omega}{K}$ and $\bar{K} = K \bar{l}$, thus the displacement $\bar{U}$ can be written

$$\bar{U} = A_j \hat{e}_j \exp\left[i K (x_i l_i - v t) \right] . \tag{26}$$

Substituting Eq. 26 into Eq. 24, we get (See Appendix A for details)

$$\left(\Gamma_{jk} - \delta_{jk} \rho_0 v^2 \right) A_j = 0 , \tag{27}$$

where $\Gamma_{jk} = \ell_i \ell_\ell C_{ijk\ell}.$

$$(28)$$

Equation 27 has non-trival solutions only if the determinant of the coefficients of A_j is equal to zero:

$$\left\| \Gamma_{jk} - \delta_{jk} \rho_0 v^2 \right\| = 0. \qquad (29)$$

Equation 29 is a cubic equation in $\rho_0 v^2$ and, therefore, we can obtain three roots or velocities v_N . The three velocities are the phase velocities of three plane waves with the same propagation direction $\mathcal{L}$. In general, the wave of largest velocity is mostly longitudinal in nature and is commonly called the quasi-longitudinal wave. The other two waves are quasishear waves.

In the study of light we have seen that only two transverse waves with different velocities can exist. Each eigen-velocity is associated with a displacement eigen vector which we calculate by substituting the eigenvelocities back into the equation for $\bar{D}$. The same technique can be used for elastic waves by substituting $\rho_0 v_N^2$ into Eq. 27. The displacement eigenvector components can be derived by solving for the ratios of A_{Nj}(See Appendix A). The normalized displacement eigenvector components are again direction cosines and are written as a_{Ni}. A plane wave of arbitrary displacement and direction $\bar{\mathcal{L}}$ will be resolved into three orthogonal displacement eigenvectors. The displacement

eigenvectors are completely uncoupled and therefore travel independently with their corresponding eigenvelocities. For a particular plane wave, the amplitudes of the displacement eigenvectors can be written as

$$\bar{A}_N = C_N \, \hat{e}_i \, a_{Ni} \tag{30}$$

where the C_N's are the displacement amplitudes into which the initial displacement has been resolved.

The three resolved plane waves can now be written by inserting Eq. 30 into Eq. 26 obtaining

$$\bar{U}_N = C_N \, a_{Ni} \, \hat{e}_i \, \exp[iK(x_j \ell_j - v_N t)]. \tag{31}$$

As in light, we should suspect that the power flow of each of the three possible plane waves for a given $\bar{K}$ is not along $\bar{K}$ and neither parallel nor perpendicular to $\bar{A}_N$. The components of the power flow across a unit surface that is normal to the crystallographic axis are derived in Appendix A, and are given as

$$P_{Ni} = \sigma_{ij} \, \dot{U}_j . \tag{32}$$

Substituting Eq. 19, Eq. 20, and Eq. 31 into Eq. 32, we get (See Appendix A)

$$P_{Ni} = \frac{1}{2} C_N^2 \, \frac{\omega}{v_N} \, c_{ijk\ell} \, a_{Nj} (\ell_\ell a_{Nk} + \ell_k a_{N\ell}). \tag{33}$$

Normalizing under the condition that $P_{N1}^2 + P_{N2}^2 + P_{N3}^2 = 1$,
we obtain the direction cosines of the energy flux or the components
of the elastic Poynting vector. The angle of deviation δ_N of the
elastic Poynting vectors $\overline{P}_N$ from the propagation vector $\overline{K}$ can
be written as

$$cos\ \delta_N = l_i\, P_{Ni} \qquad (34)$$

where P_{Ni} in this equation are the direction cosines. The
magnitude of the ray vector can be calculated from

$$\upsilon_{N(RAY)} = \frac{\upsilon_N}{cos\ \delta_N} \qquad . \qquad (35)$$

The velocity of the disturbance which carries the energy is
called the ray velocity and, as in light, the wavesurface can
be constructed by plotting all possible endpoints of the ray
vector. In Fig. 6 an example is given of such surfaces for
elastic waves in aluminum.
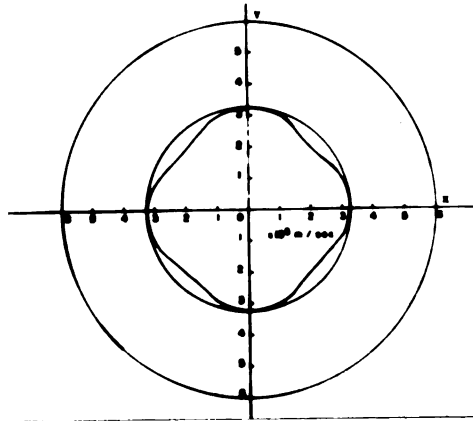
Figure 6. **Wave surfaces of aluminum.**

For light the deviation angles of the power flow from
the wave normals are at most a few degrees; but, for elastic waves,
deviations can be as much as a radian. The deviation of power flow
for a plane wave propagating in the direction of ∧**the** y-axis in quartz
was numerically calculated to be about 25 degrees for all three
waves.

For this specific case, the results of an experiment[9]
which renders the sound beam visible will be used to illustrate
the properties of eigenvelocities, displacement eigenvectors, and
the ray deviation. Figure 7 shows the direction of power flow and
the wavefronts of a quasilongitudinal and a quasishear elastic wave.

In order to fully interpret the photographs of Figure 7,
a short review of the case of a plane wave propagating along the
Y-axis in a sample of quartz is appropriate. Figure 8 shows two
displacement eigenvectors and their associated power flow direc-
tions as calculated from known elastic constants. The third dis-
placement eigenvector is out of the page and its associated power
flow is close to power flow of the shown quasishear wave.

If a displacement is imposed along the Y-axis, as for
example, by an X-cut quartz transducer which is mounted on a
surface perpendicular to the Y-axis, two modes of displacement
can be excited simultaneously. The transducer does not have a
displacement component along the X-axis and therefore no motion
is resolved in the direction the eigenvector which is directed
along the X-axis. The quartz-air interface on the right side of
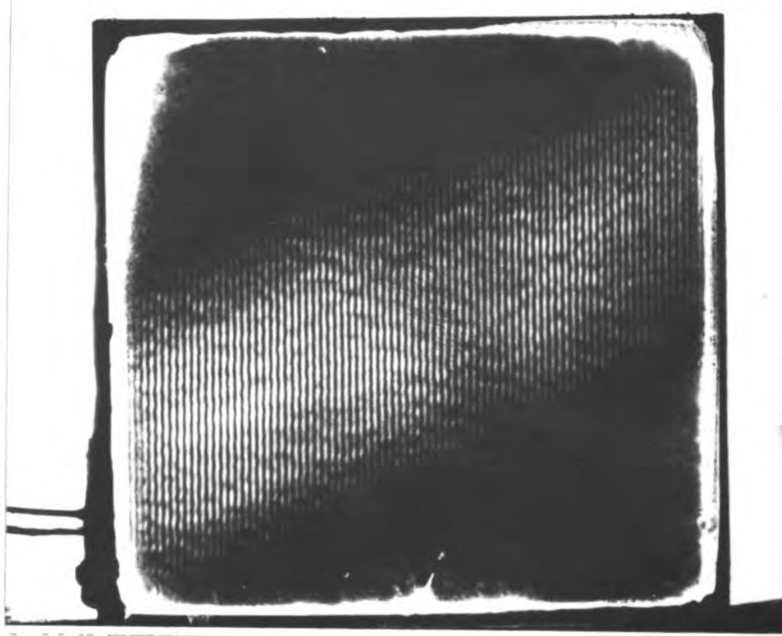
(a)
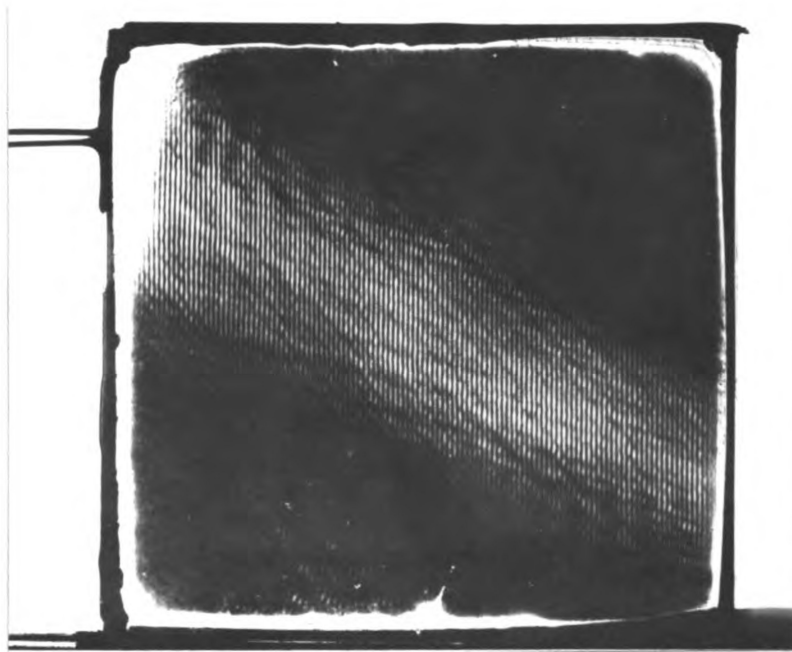
(b)

Figure 7.   Photographs showing the wavefronts and power flows of quasilongitudinal (a) and quasishear (b) waves in quartz.
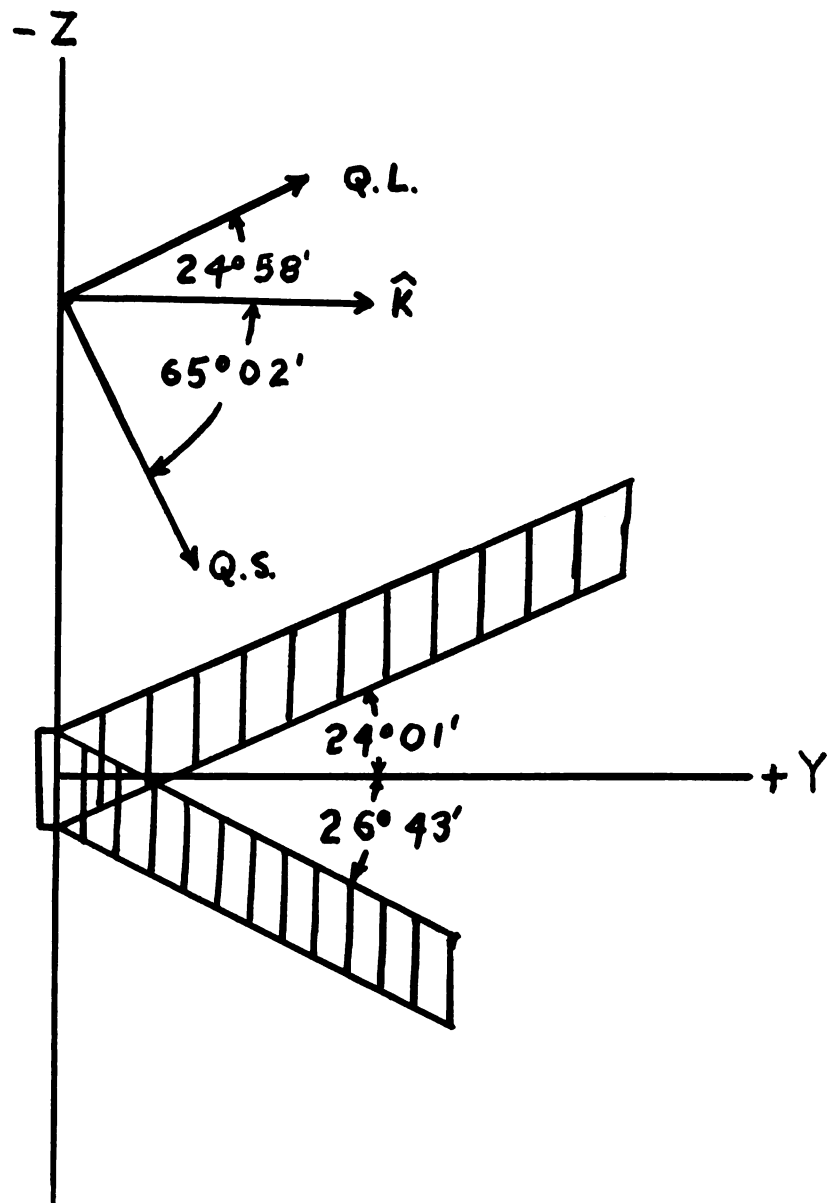
Figure 8. Schematic diagram of the displacement eigenvector and directions of power flow for an elastic wave propagating in the direction of the y-axis in quartz.

Figure 7 reflects the two sound beams back along the same paths which they have traveled before reflection. By adjusting the driving frequency of the transducer, a stationary wave can be established. It is these two stationary waves that are rendered visible in Figure 7.

In the lower left of Fig. 7a the outline of the x-cut quartz transducer, whose motion is along the y-axis, can be seen. This figure shows the quasilongitudinal mode with its wavefronts and power flow clearly visible. The motion of the x-cut transducer is, of course, resolved into a longitudinal wave and a transverse or shear wave. The energy flow of the quasishear wave is downward and, therefore, is reflected about and eventually dissipated. Consequently, this shear wave has no chance to develop sufficient amplitude to be visible. The longitudinal beam is spreading and therefore fills up every possible space for this mode. The upper left and lower right triangular regions of the block contain no sound due to reflection from the upper and lower surfaces. If we move the transducer to the upper corner, a longitudinal resonance is now impossible because it would be reflected about as the quasishear wave is in Fig. 7a; however, the shear mode can be tuned to resonance. Figure 7b shows the quasishear mode in resonance. Due to the lower velocity of the quasishear mode, the separation of the wavefronts is less.

In Chapter II, the electrical equivalent quantities were derived as in this chapter. From those quantities, the normal velocity surface, the wave surface, and the concept of

point sources and plane waves in Huygens' construction were developed. Since the latter mentioned concepts are identical for elastic waves, no discussion is necessary but only a short comparison is appropriate. Of course, due to the greater complexity of elastic waves compared to electromagnetic waves, additional anomalies are found, and they will be discussed in the next chapter.

The question whether Huygens' construction and its consequences are valid for elastic waves can, to some extent, be answered by comparing our numerical results with numerical results given by Musgrave[6,7] who used Huygens' construction as the foundation for his expressions. Musgrave transformed Eq. 27 into a form which can be interpreted as the analytical expression of the normal velocity surface. By studying Fig. 5, we can see that the wave surface can be graphically obtained from the normal velocity surfaces by using Huygens' construction. Musgrave[10] derived an analytic expression for the points on the wave surfaces by using the equations of the normal velocity surfaces and the equations required for constructing the tangent surfaces. Those points on the wave surface belong to a particular plane wave propagation vector and therefore give the ray velocities and ray directions directly. Musgrave calculated by his method the normal velocity surfaces and the wave surfaces for some crystals of cubic[7] and hexagonal[6] symmetry. In Appendix C, a computer program is described which numerically calculates all necessary quantities with the equations given in this chapter. The expressions given in this

chapter and the expressions given by Musgrave are mathematically

of different form. Since it is not completely obvious by looking

at the two forms that they will give the same numerical results,

several surfaces previously calculated by Musgrave were recalcu-

lated for comparison. As expected, the results were identical

and, therefore, both methods are compatible for calculating the

direction of energy flow. The use of wave surfaces and Huygens'

principle should give us valuable clues to the behavior of elastic

waves. Fig. 6 shows such surfaces for aluminum. Its behavior is

close to isotropic and therefore the surfaces are smooth and simple.

More complicated surfaces are discussed in the next section.

CHAPTER IV

SPECIAL TOPICS

A. Wave Surfaces With Cuspidal Edges

A wave surface can be interpreted as the surface which
describes the boundary between the disturbed and undisturbed region
due to a wave emanating from a point source. For light, the wave
surfaces are either of one sheet or, in general, at most of two
sheets. As two wave surfaces are possible, in general, a flash from
a point source would result in two flashes when observed through an
anisotropic material far away from the source. From Fig. 6, we can
see that elastic waves have three wave surfaces and, therefore, we
would receive three pulses from a single pulse originating from a
point. If we look caredully at the wave surfaces shown in Fig. 9
and 10, we see cuspidal edges on the wave surfaces of one shear mode.
Observation in the angular regions of the cuspidal edges will result
in the reception of as many as five pulses rather than the normal
three. This peculiar phenomenon usually occurs when the deviation
of the power flow is large. A detailed study of cuspidal edges has
been given by Musgrave[8].

We can use Huygens' construction to illustrate what happens
when we consider plane waves rather than a point source. Using the
techniques previously explained for Fig. 5, we have explored the
bicuspidal edges on the wavesurface of KBr. In this example, the
bicuspidal edge in the [001] plane is symmetric about the <110>
direction. In Fig. 11, we have drawn tangent lines to the wave-

(a)   (b)
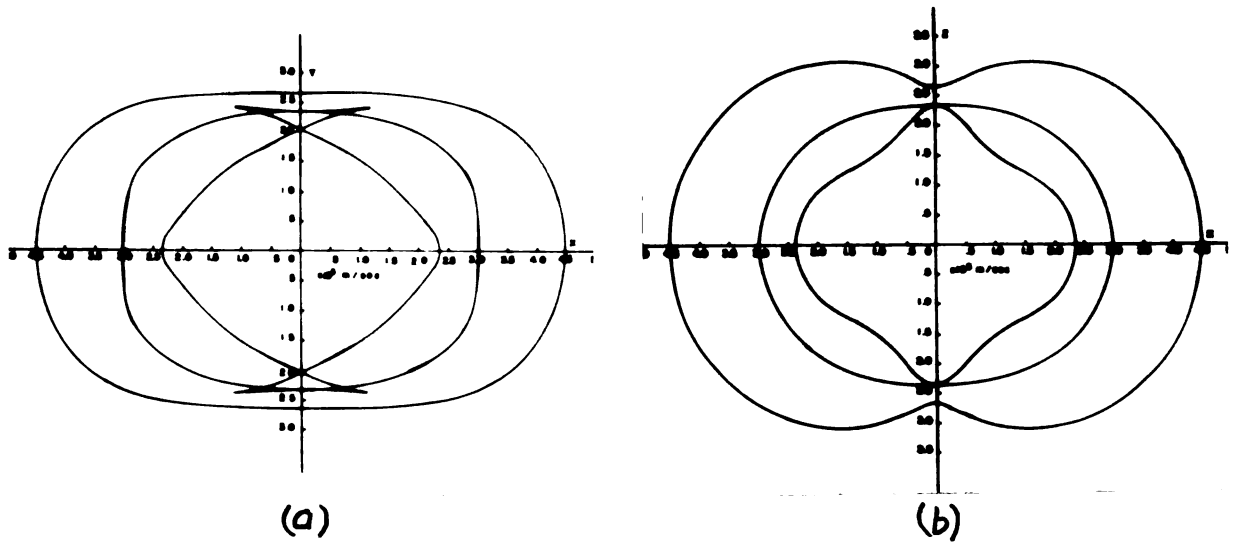
Figure 9. **Wave surfaces (a) and normal velocity surfaces (b) of zinc.**

(a)   (b)
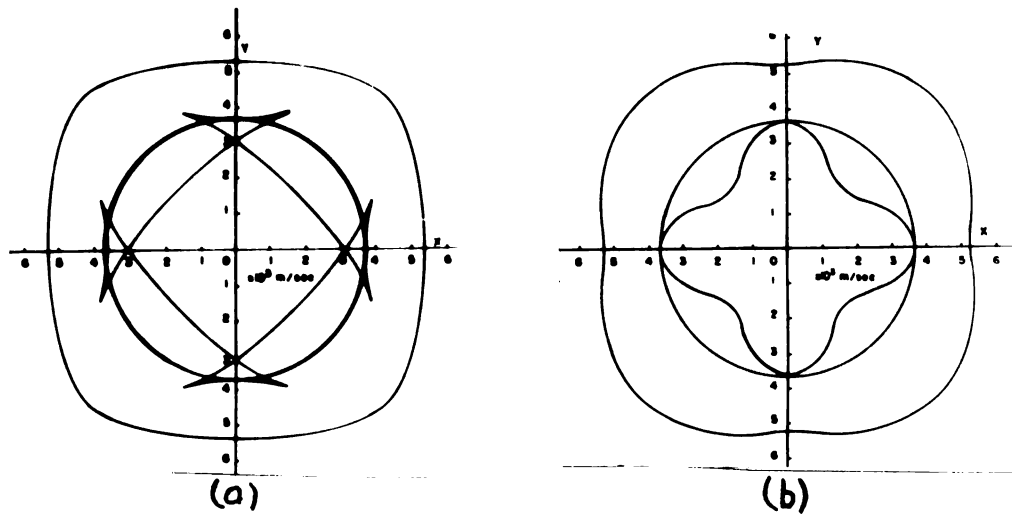
Figure 10. **Wave surfaces (a) and normal velocity surfaces (b) of nickel.**
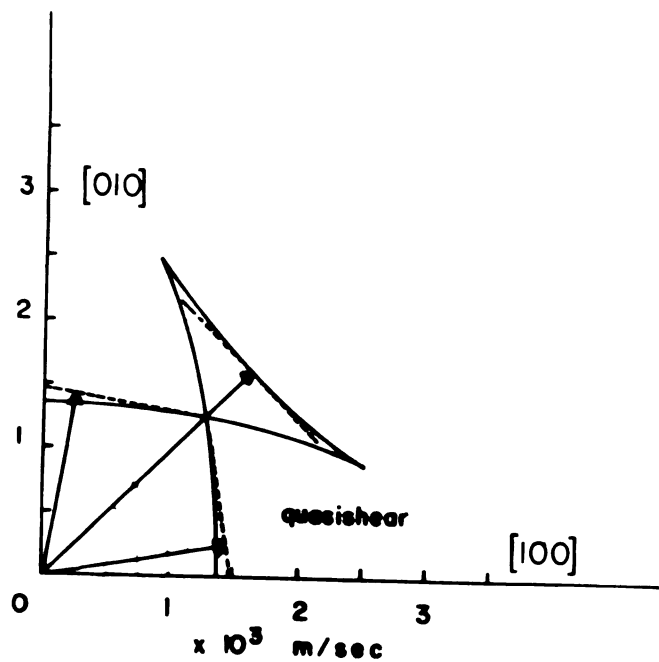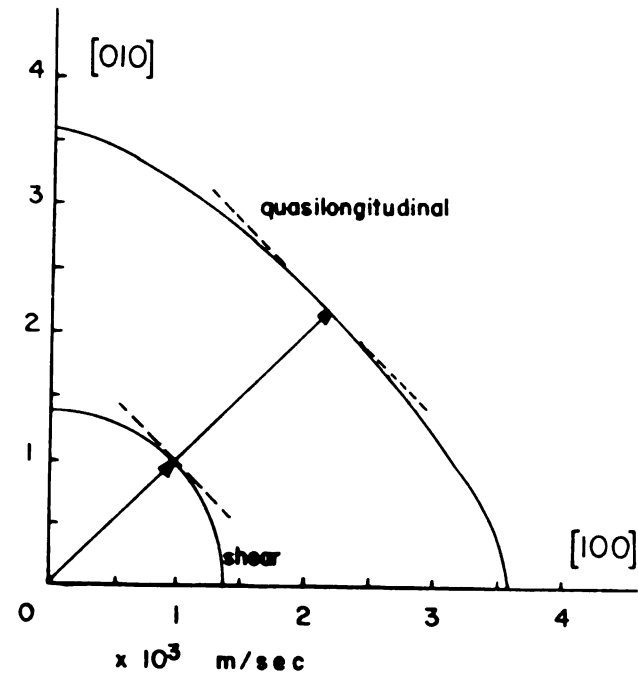
Figure 11. <u>Graphical construction of the normal velocities and the direction of the propagation vectors of plane waves which have power flows in the [110] direction of KBr.</u>

surfaces at every point where a surface crosses the 110 direction. The normal velocities and direction of the propagation vectors were then ascertained by constructing perpendicular intersectors which also passed through the origin. We find that five waves have their power flow in a particular 110 direction: namely, three wave (one longitudinal and two shear) with wave normals in the 110 direction, and two other shear waves whose respective propagation directions are approximately 10° and 80° from the 100 direction. Hence, the bicuspidal edges on wavefronts can be interpreted to mean that more than one plane wave have their power flows in the same direction.

Using the approximate values given above as a guide, better values for the propagation direction with power flow in the 110 direction were found by calculating the direction of power flow for several propagation directions about nearly 10° from the axis. These desired propagation directions were found to be 8.9° and 81.1° respectively.

B. Graphical Representation of Power Flow

It is now clear that wave surfaces are able to describe elastic wave behavior in a material qualitatively; however, quantitatively they are not too useful except for approximate values. Another limitation is the difficulty of representing them in three dimensions. In order to portray elastic wave behavior more accurately in three dimensions, several graphical techniques have been

devised[11]. Figure 12 is an example of a graph which can be used
to present the direction of the power flow or the displacement
eigenvector for a particular mode in a specific material. Figure
12 shows the power flow of the quasilongitudinal mode in quartz.
This graph gives a good overall view of energy flow of one mode
in a specific material. The square grid represents the power flow
direction of the longitudinal wave and the superimposed grid repre-
sents the direction of the propagation vector $\widetilde{K}$. If $\widetilde{K}$ is known
and plotted on the superimposed grid, this point read from the
square grid will give the direction of the power flow. The
reverse procedure can be used if the direction of the power flow
is known or if a particular beam direction is desired.

C. Conical Refraction

In optical biaxial crystals, light exhibits a peculiar
phenomenon, known as conical refraction. An investigation of this
phenomenon in light can be extended to elastic waves. By analyzing
the wave surfaces of optical biaxial crystals, it is found that
there are four directions where the intersection of the wave sur-
faces resembles the top of a volcano. Figure 13a shows the cross-
section of a hypothetical wave surface (this is a construct for
explanation only). If a plane wave of single propagation direc-
tion $\widetilde{K}_0$ were possible, the surface normal to $\widetilde{K}_0$ would touch
the entire rim of the volcano-like wave surfaces. In the case
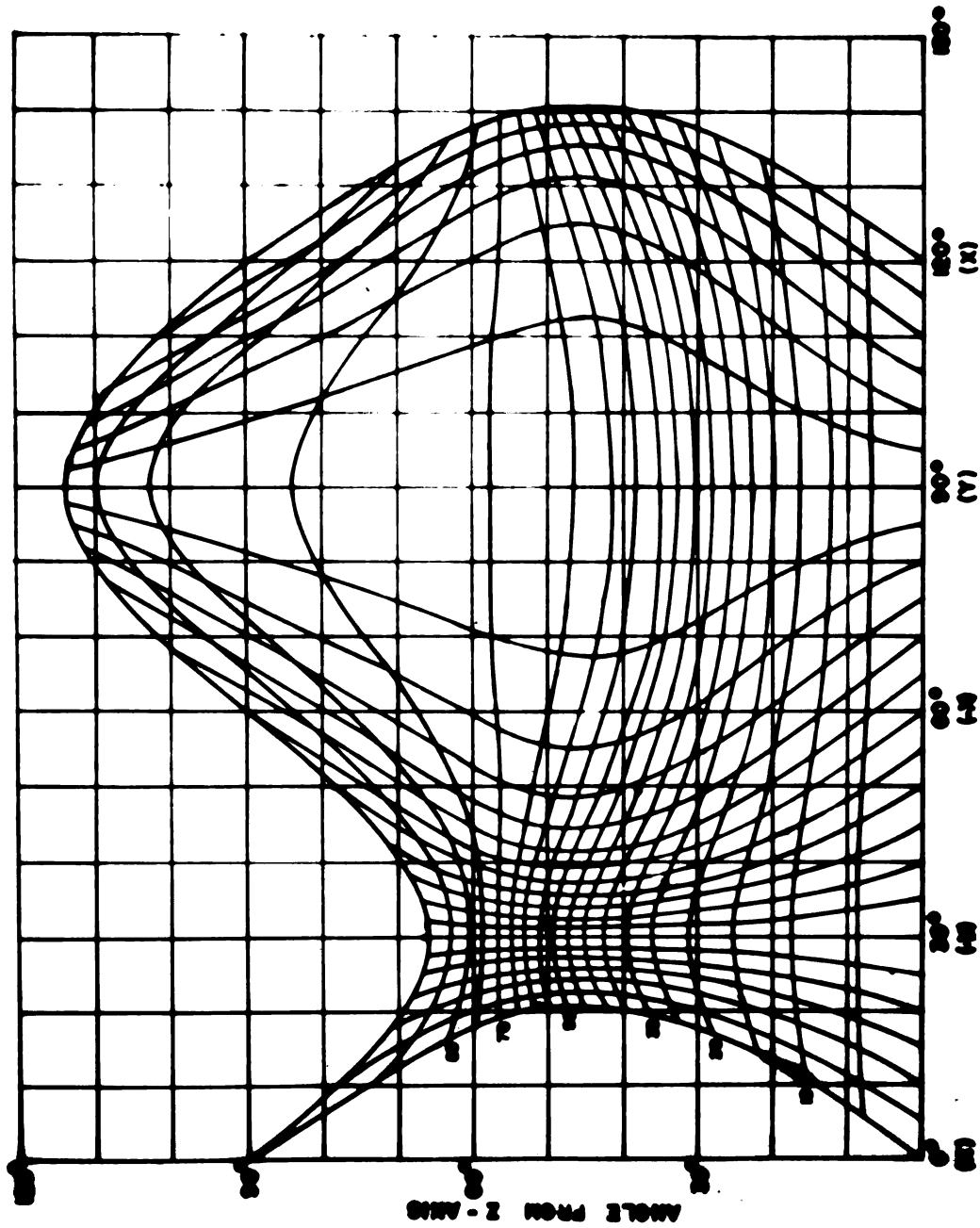
Figure 12. Graphical representation of power flow of the quasilongitudinal mode in quartz.
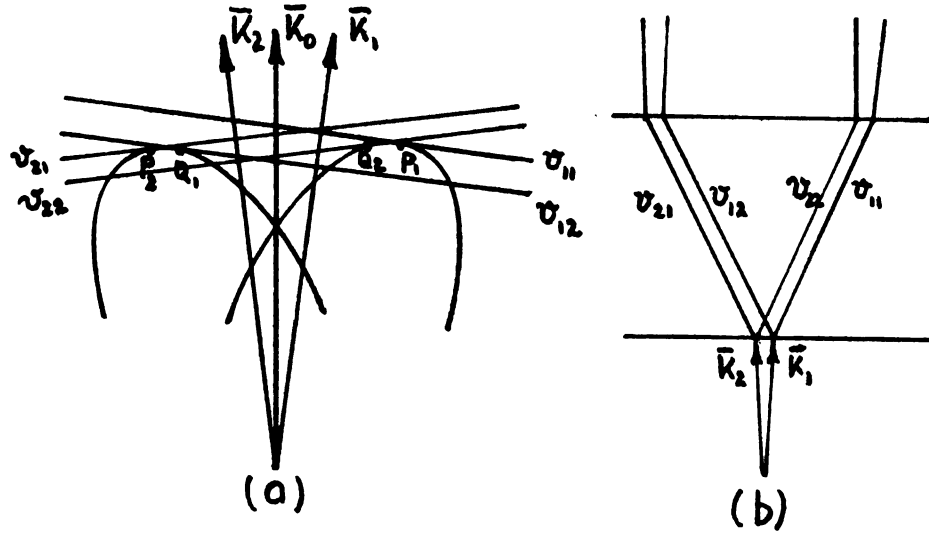
Figure 13. **Conical refraction of light in biaxial
crystals.** (a) shows the cross section of
intersecting wave surfaces which gives
rise to conical refraction. (b) shows
the power flow of two slightly off axis
wavevectors.

where the propagation vectors deviate greatly from $\overline{K}_0$, as $\overline{K}_1$

and $\overline{K}_2$ shown in Fig. 13, the energy would flow, according to

Huygens' construction, to the points P_1 and Q_1 for $\overline{K}_1$ with

normal velocities υ_{11} and υ_{12} respectively and for $\overline{K}_2$ to the

points P_2 and Q_2 with normal velocities υ_{21} and υ_{22} respectively.

If we let $\overline{K}_1$ and $\overline{K}_2$ approach $\overline{K}_0$, the points P_1 and Q_2 and

P_2 and Q_1 will be nearly at the same position and the normal

velocities will approach each other. Any finite beam of light

which propagates along $\overline{K}_0$ will consist of an infinite number of

plane waves whose propagation vector is very nearly $\overline{K}_0$. Under ordinary conditions, a narrow pencil of light can be achieved at best. In Fig. 13b, the power flows of the two propagation vectors are shown. A pencil of light will produce an entire cone of light.

The identical conditions are present in certain directions in anisotropic materials for transverse elastic waves. These conditions are met along trigonal axes such as in the z-direction of quartz or in the $\langle 111 \rangle$ directions in certain cubic crystals. For the above directions, the cone is circular, but in other special directions where conical refraction occurs the cross section of the cone is not necessarily circular. With the computer program in the appendix, calculations have been made for conical refraction occuring about the z-direction for quartz. The displacement eigen-vectors and the power flows have been computed and plotted in Fig. 14 for propagation vectors which are .01 degrees off the z-axis.

Each $\hat{K}$ vector has two shear modes with their power flows nearly 16.8° from the z-axis. In Fig. 14, the surface of a unit sphere is mapped into the plane of the paper with its pole (z-axis) pointing out of the paper. Points in this plane represent endpoints of vectors with their origin at the center of the sphere. The endpoints of the $\hat{K}$ vectors all lie on the dashed circle and their corresponding power flow lie on the solid circle. Some typical $\hat{K}$ vectors are shown as solid and open dots on the dashed circle. The intersections of the line which passes through the
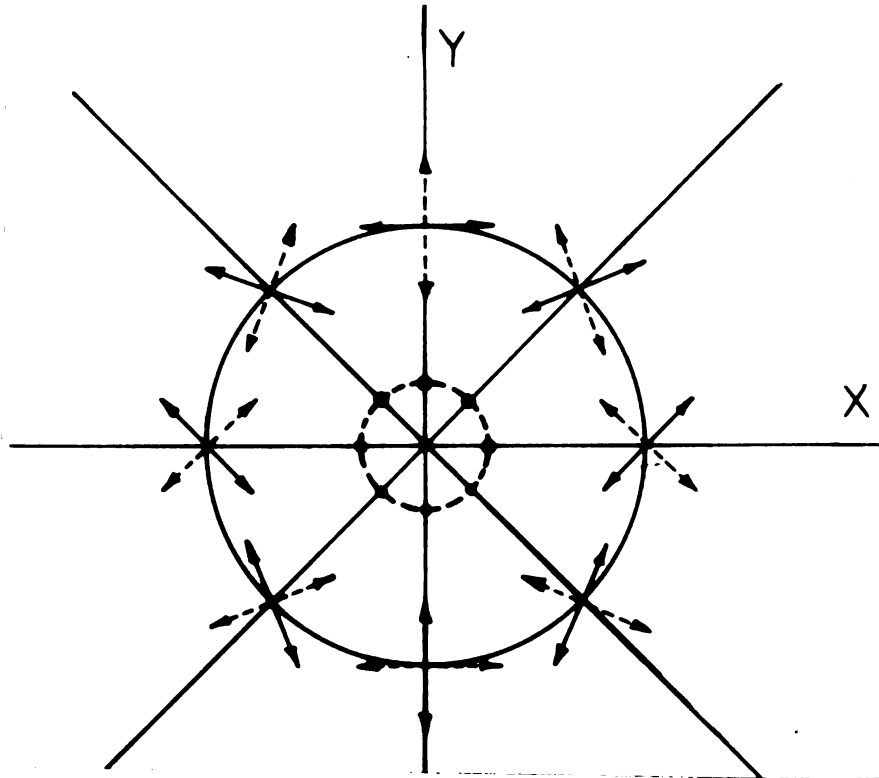
Figure 14. **Conical refraction in quartz.**

pole and the endpoint of a particular $\hat{K}$ vector with the solid

circle gives the corresponding power flow vectors. On the end-

points of the power flow vectors, the corresponding displacement

eigenvectors, all which lie in the xy-plane, are shown as arrows.

The solid and dashed arrows correspond to solid and open dots,

respectively. The direction of the power flow and the displace-

ment vectors are very insensitive to small angular changes of the

propagation vector $\hat{K}$ from the z-axis. Any finite source will

have a distribution of $\hat{K}$ vectors about the z-axis and, there-

fore, the power will flow to all points on the solid circle.

In summation, I would like to point out that, in general,

observed light propagation phenomena in anisotropic media are a

result of the decomposition of a wave of arbitrary polarization

into two eigenpolarizations which travel independently, with

different normal velocities and ray directions. As we have seen,

this is also the case in sound, and, therefore, the method of

analysis used in studying optical problems, such as ordinary

refraction, conical refraction, reflection, circular and el-

liptical polarization, interference, etc., and can be directly applied

to elastic waves.

APPENDIX A

MATHEMATICAL DETAILS FOR ELASTIC WAVE PROPAGATION

In this appendix we develop the details which are necessary in order to make proper use of the computer program in Appendix C; at the same time, the theory outlined in Chapter III is worked out in full. While going through the mathematical steps, reference to the computer program is made by giving the range of card numbers in double brackets as ((27-34)). These cards will be the computer program's equivalent mathematical steps. Equation 24, which is the wave equation of an anisotropic, linear homogeneous solid is written as follows:

$$\rho_0 \, \ddot{U}_j = \frac{1}{2} C_{ijkl} \, \frac{\partial}{\partial x_i} \left(\frac{\partial U_k}{\partial x_l} + \frac{\partial U_l}{\partial x_k} \right). \tag{A1}$$

The solution assumed for the above wave equation is a plane wave $\bar{U}$, (Eq. 25) where

$$\bar{U} = A_i \, \hat{e}_i \, \exp[i K (x_j \ell_j - v t)]. \tag{A2}$$

Differentiating Eq. A2, we obtain

$$\frac{\partial U_j}{\partial x_i \, \partial x_l} = - U_j \, K^2 \, \ell_i \ell_l , \tag{A3}$$

and

$$\ddot{U}_j = - U_j \, K^2 v^2. \tag{A4}$$

Substituting Eq. A3 and Eq. A4 into Eq. A1, we find

$$\rho_0 v^2 K^2 U_j = \tfrac{1}{2} C_{ijkl} K^2 \ell_i (\ell_l A_k + \ell_k A_l) \ell^\eta, \qquad (A5)$$

where

$$\eta = i K (x_j \ell_j - v t).$$

Dividing by $K^2 \ell^\eta$, the above equation becomes

$$\rho_0 v^2 A_j = \tfrac{1}{2} C_{ijkl} \ell_i (\ell_l A_k + \ell_k A_l). \qquad (A6)$$

Since $C_{ijkl}(\ell_k A_l)$ is equivalent to $C_{ijlk}(\ell_l A_k)$, Eq. A6 can be rewritten as

$$\rho_0 v^2 A_j = \tfrac{1}{2} \ell_i \ell_l (C_{ijkl} + C_{ijlk}) A_k \qquad (A7)$$

Defining a new variable, namely

$$\Gamma_{jk} = \ell_i \ell_l C_{ijkl}, \qquad (A8)$$

and noting that $C_{ijkl} = C_{ijlk}$, Eq. A6 can be rewritten as

$$(\Gamma_{jk} - \rho_0 v^2 \delta_{jk}) A_k = 0. \qquad (A9)$$

The above has non-trivial solutions only if the determinant of the coefficients is equal to zero:

$$\left\| \Gamma_{jk} - \rho_0 v^2 \delta_{jk} \right\| = 0, \qquad (A10)$$

or

$$
\begin{Vmatrix}
\Gamma_{11} - \rho_0 v^2 & \Gamma_{12} & \Gamma_{13} \\
\Gamma_{12} & \Gamma_{22} - \rho_0 v^2 & \Gamma_{23} \\
\Gamma_{13} & \Gamma_{23} & \Gamma_{33} - \rho_0 v^2
\end{Vmatrix} = 0 .
$$

The above is a cubic equation in $\rho_0 v^2$ and therefore has three

roots. The three roots are the eigenvelocities which are associated

with three eigenvectors. The numerical calculations are made in

the computer program from card 45 through 93.

Substituting the eigenvelocities into Eq. A9, we obtain

$$
\begin{vmatrix}
\Gamma_{11} - \rho_0 v_N^2 & \Gamma_{12} & \Gamma_{13} \\
\Gamma_{12} & \Gamma_{22} - \rho_0 v_N^2 & \Gamma_{23} \\
\Gamma_{13} & \Gamma_{23} & \Gamma_{33} - \rho_0 v_N^2
\end{vmatrix}
\begin{vmatrix}
A_{N1} \\
A_{N2} \\
A_{N3}
\end{vmatrix} = 0 . \tag{A11}
$$

To calculate the three components of the three eigenvectors, we

solve Eqs. A11 simultaneously for the ratio's of the A_{Ni}'s.

One of the three possible forms of ratio's β_i is written as follows: ((94-106)):

$$\beta_1 = \frac{A_{N1}}{A_{N1}} = 1 \qquad ;$$

$$\beta_2 = \frac{A_{N2}}{A_{N1}} = \frac{\Gamma_{23}(\Gamma_{11} - \rho_0 v_N^2) - \Gamma_{12}\Gamma_{13}}{\Gamma_{13}(\Gamma_{22} - \rho_0 v_N^2) - \Gamma_{12}\Gamma_{23}} \qquad ; \qquad \text{(A12)}$$

$$\beta_3 = \frac{A_{N3}}{A_{N1}} = \frac{\Gamma_{23}(\Gamma_{11} - \rho_0 v_N^2) - \Gamma_{12}\Gamma_{13}}{\Gamma_{12}(\Gamma_{33} - \rho_0 v_N^2) - \Gamma_{23}\Gamma_{13}} \qquad .$$

If two or all off-diagonal terms of Γ are zero, as is the case if $\bar{K}$ is along the crystal axis, the above ratios are indeterminate. Therefore, we must test for that condition ((57)) and proceed to solve Eqs. A11 in a different way. From Eq. A10, we can see that if all off-diagonal terms are zero, it follows that $\Gamma_{11} = \rho_0 v_1^2$, etc., and the displacements are along the corresponding crystal axis ((132-138)). If only one off-diagonal term is non-zero, we obtain one $\rho_0 v_N^2$ immediately with the corresponding $A_{N\lambda}$ being along a coordinate axis. The remaining nonzero minor will be a quadratic equation in $\rho_0 v^2$. Substituting the two roots of the quadratic equation into Eqs. A11 and nothing that the component of the pure displacement vector found initially will be set to zero, we obtain the ratios of the $A_{N\lambda}$'s by solving Eqs. A11 simultaneously ((106-132)).

In order to obtain the eigendisplacement direction

cosines a_{Ni} , we must normalize by $a_{Ni} = \beta_i / (\beta_s^2)^{\frac{1}{2}} ((139-145))$.

The direction of power flow in an anisotropic material can be obtained by considering the energy change in a finite volume per unit time. The energy change per unit time must be equal to the power flow out of the volume. If the components of power flow out of the volume are considered to be along the coordinate axes across a unit area, the elastic equivalent to the Poynting vector can be obtained.

If W is the potential energy per unit volume, the stress can be written as

$$\frac{\partial W}{\partial \epsilon_{ij}} = \sigma_{ij} \quad , \tag{A13}$$

or

$$dW = \sigma_{ij} \, d\epsilon_{ij} = C_{klij} \, \epsilon_{ij} \, d\epsilon_{ij} . \tag{A14}$$

Therefore, we find

$$W = C_{klij} \int_0^{\epsilon_{ij}} \epsilon_{ij} \, d\epsilon_{ij} = \frac{1}{2} \sigma_{ij} \, \epsilon_{ij} . \tag{A15}$$

The total energy per unit volume is the sum kinetic energy T and potential energy W , or

$$E = T + W = \frac{1}{2} \rho_0 \dot{u}_j^2 + \frac{1}{2} \sigma_{ij} \, \epsilon_{ij} . \tag{A16}$$

The rate of change of energy in the unit volume can be obtained

by differentiating (Eq. A16) with respect to time,

$$\dot{E} = \rho_0 \ddot{U}_j \dot{U}_j + \tfrac{1}{2} \dot{\sigma}_{ij} \epsilon_{ij} + \tfrac{1}{2} \sigma_{ij} \dot{\epsilon}_{ij} \tag{A17}$$

The last two terms can be shown to be equal by use of Hooke's

law. From Eq. 22, $\rho_0 \ddot{U}_j$ can be rewritten and substituted into

Eq. A16, resulting in

$$\dot{E} = \frac{\partial \sigma_{ij}}{\partial x_i} \dot{U}_j + \sigma_{ij} \frac{\partial \dot{U}_i}{\partial x_i} = \frac{\partial}{\partial x_i} \left(\sigma_{ij} \dot{U}_j \right). \tag{A18}$$

The total energy change in a finite volume can thus be written

as

$$\dot{E}_v = \int_v \frac{\partial}{\partial x_i} \left(\sigma_{ij} \dot{U}_j \right) d\tau. \tag{A19}$$

Converting this integral into a surface integral by use of the

divergence theorem, we get

$$P_i = \dot{E}_{vi} = \int_{\beta_i} \sigma_{ij} \dot{U}_j \, d\beta_i, \tag{A20}$$

where β_i is the component of surface area normal to the

direction i. Thus the elastic equivalent to the Poynting vector

is

$$P_i = \sigma_{ij} \dot{U}_j. \tag{A21}$$

Substituting Eq. 17 and Eq. 19 into Eq. A21, we obtain

$$P_{Ni} = \frac{1}{2} C_{ijkl} \left(\frac{\partial U_{Nk}}{\partial x_l} + \frac{\partial U_{Nl}}{\partial x_k} \right) \dot{U}_{Nj} . \qquad \text{(A22)}$$

From Eq. 30, the incident plane wave has been resolved into displacement eigenvectors, where three plane waves were obtained of the form

$$U_{Ni} = C_N a_{Ni} \hat{e}_i \exp \left[i K_N (x_j l_j - v_N t) \right] . \qquad \text{(A23)}$$

Taking the time and space derivatives of Eq. A23, we obtain

$$\dot{U}_{Nj} = - i K_N C_N a_{Nj} e^{n} , \qquad \text{(A24)}$$

and

$$\frac{\partial U_{Nk}}{\partial x_l} = i K_N C_N l_l a_{Nk} e^{n} . \qquad \text{(A25)}$$

Substituting Eq. A24 and Eq. A25 into Eq. A22, we find that

$$P_{Ni} = \frac{1}{2} C_N^2 K_N^2 v_N^4 a_{Nj} (a_{Nk} l_l + a_{Nl} l_k) e^{2n} . \qquad \text{(A26)}$$

Time-averaging Eq. A26 over one cycle and noting that $v_N = \frac{\omega}{K_N}$ we obtain

$$P_{Ni} = \frac{1}{2} C_N^2 \frac{\omega^2}{v_N} C_{ijkl} a_{Nj} (a_{Nk} l_l + a_{Nl} l_k) .$$

Equation A27 gives us the elastic Poynting vector with the components of power flow across unit area in the direction of the crystal axes. The numerical calculations have been accomplished in the computer program by card number 146 through 156 and the normalization is accomplished by card numbers 157 through 161.

The normal velocity ϑ_N is calculated from $\rho_0 \vartheta_N^2$ by cards 161 and 163.

APPENDIX B

INSTRUCTIONS FOR THE USE OF THE COMPUTER PROGRAM

The program, written Fortran II, calculates:

1) The directions of the displacement eigenvectors,

in terms of   a)   direction cosines,

b)   angles in spherical coordinates.

2) The direction of the associated power flow,

(ray direction) in terms of

a)   direction cosines

b)   angles in spherical coordinates.

3) The deviation of the ray direction from the plane

wave normal.

4) The normal and ray velocities.

The input necessary for calculating these quantities

is:

1) The elastic constants of the material,

2) The density of the material,

3) The direction of propagation of the desired elastic

plane wave.

INPUT

The input is achieved in the following sequence:

Card	Field	Format	Explanation
1	1	5A8	Reads the program name
2-10	1-9	9F7.4	Inputs the elastic constants. Table I lists the elastic constants in sequence as they are read.

Card	Field	Format	Explanation
11	1	F10.3	Inputs density of material in kg/m^3.
11	2	F7.1	Inputs the divisor by which the numbers of fields 3 through 9 are divided. The result of this division is the conversion of these numbers into degrees of angle.
11	3-5	316	Reads the angles of the propagation vector in spherical coordinates. Field 3-6 determine the angle θ, with starting angle, angle limit, and angle steps listed, respectively.
11	6-9	316	Angles $\emptyset$ in spherical coordinates are read in the same way as the angle θ. The angle $\emptyset$ goes through all its values before another value is taken of the angle θ.
11	10	316	The following three numbers (one in each field) define the reference axes for the angles θ and $\emptyset$. 1 2 3 ....$\emptyset$ is rotated in the xy-plane measured from the x-axis toward the y-axis. θ is referred from the z-axis.

Card	Field	Format	Explanation
			132 ....$\emptyset$ is rotated in the xz-plane measured from the x-axis toward the z-axis. θ is referred from the y-axis.
			2 3 1 .....$\emptyset$ is rotated in the yz-plane measured from the y-axis toward the z axis. θ is referred from the x-axis.
11	11	16	The following code numbers give continuation instructions: 0....stop the program. 1....repeat card 11 with different data. 2....read in new set of cards as cards 1-11 with new data.

OUTPUT

For every set of calculations the direction of the propagation vector is specified in the heading.

There are three major columns, each containing the calculated quantities for one mode with its associated eigenvelocity given in the last line. The abbreviations at the

TABLE I

Fields (F7.4)

Cards	1	2	3	4	5	6	7	8	9
2	11	16	15	16	12	14	15	14	13
3	16	66	56	66	26	46	56	46	36
4	15	56	55	56	25	45	55	45	35
5	16	66	56	66	26	46	56	46	36
6	12	26	25	26	22	24	25	24	23
7	14	46	45	46	24	44	45	44	34
8	15	56	55	56	25	45	55	45	35
9	14	46	45	46	24	44	45	44	34
10	13	36	35	36	23	34	35	34	33

The numbers in the Table are the subscripts of
the elastic constants, e.g., on card 5, field 6,
46 indicates the value of the elastic constant C_{46}
should be inputted. (For details concerning four
to two subscript conversion see Nye[11])

beginning of each line indicate the following quantities:

DVDC....Displacement vector given in direction
cosines showing the x,y and z components
respectively.

DVDG....Displacement vector given in spherical
coordinates. The first angle is measured
from the x-axis and the second from the z-axis.

PVDG....Elastic Poynting vector given in

direction cosines (same order as in

DVDC).

PVDG....Elastic Poynting vector given in sper-

ical coordinates (same order as in

DVDG).

RVDV....Ray velocity and ray deviation in

m/sec and degrees, respectively.

PLWV....Plane wave phase velocity.

As a sample problem, let us calculate the quantities which are necessary to plot Fig. 12. The material is quartz and, therefore, we name the program QUARTZ CRYSTAL as shown in sample data card 1. Nye[11] lists the nonzero terms and equivalent values of the elastic constants for crystal class of symmetry 32 (such as alpha quartz). The following relationships between the constants were given:

$$c_{11} = c_{22}$$

$$c_{33} = c_{33}$$

$$c_{44} = c_{44}$$

$$c_{66} = 1/2(c_{11} - c_{12})$$

$$c_{12} = c_{12}$$

$$c_{13} = c_{23}$$

$$c_{14} = c_{56} = -c_{24}$$

All other constants are zero.

The numerical values of the constants as given by Farnell[12]
are

$$c_{11} = .8694$$

$$c_{33} = 1.0680$$

$$c_{44} = .5762$$

$$c_{12} = .0696$$

$$c_{13} = .1560$$

$$c_{14} = .1743 \ .$$

These numerical values are shown in sample cards 2 - 10.
Taking symmetry into account, we need only to vary the angle θ
through 90 degrees from the z-axis and the angle $\emptyset$ through 120 degrees
in the xy-plane in order to obtain the overall power flow behavior
in a sample of quartz. The incremental angle was chosen to be
5 degrees. Sample data card 11 shows these instructions for θ and
$\emptyset$.

It is recommended that several features of the program
be changed or deleted if other information is required. The refer-
ences in the theory of Appendix A, the cross reference and the flow
chart in Appendix C should enable such changes to be made without
much difficulty. For greater precision in the calculated results,
the program should be changed to double precision. By adding a
plot routine to the program, wave surfaces, angles of deviation
and many other parameters may be plotted.

COMPUTER PROGRAM

```
      ODIMENSION C1(3,3,3),C2(3,3,3),C3(3,3,3),D(3),G(3,3),V(3),S(3,3),      1
     1DC(3,3),SNORM(3),T(3.3),B(3),THETA1(3),FEE1(3),THETA2(3),FEE2(3),
     2DIVIDE(3),RAYV(3),DEV(3)
  101 READ 103, INFO1,INFO2,INFO3,INFO4,INFO5
  104 DO 10 J=1,3                                                            5
      READ 106, ((C1(J,K,L),L=1,3),K=1,3)
      READ 106, ((C2(J,K,L),L=1,3),K=1,3)
   10 READ 106, ((C3(J,K,L),L=1,3),K=1,3)
      DO 201 J=1,3
      DO 201 K=1,3                                                          10
      DO 201 L=1,3
      C1(J,K,L)=C1(J,K,L)*1.E11
      C2(J,K,L)=C2(J,K,L)*1.E11
  201 C3(J,K,L)=C3(J,K,L)*1.E11                                             15
 3200READ 609, ROW, DIV, NSTRT1,NLIM1.NSTEP1,NSTRT2,NLIM2,NSTEP2,IP,JP,KP,
     1NOW
      PRINT 610
      PRINT 128, INFO1,INFO2,INFO3,INFO4,INFO5
      PRINT 388,IP,JP,KP                                                    20
      NSTRT1=NSTRT1+1
      NSTRT2=NSTRT2+1
      NLIM1=NLIM1+1
      NLIM2=NLIM2+1
      DO 300 ID=NSTRT1,,NLIM1,NSTEP1                                        25
      DO 300 JD=NSTRT2, NLIM2,NSTEP2
      DEG1=ID-1
      DEG2=JD-1
      DEG1=DEG1/DIV
      DEG2=DEG2/DIV                                                         30
      RAD1=DEG1*.01745329
      RAD2=DEG2*.01745329
      D(IP)=COSF(RAD2)*SINF(RAD1)
      D(JP)=SINF(RAD1)*SINF(RAD2)
      D(KP)=COSF(RAD1)                                                      35
      GO TO 111
  331 PRINT 749,DEG2,IP,DEG1,KP
      PRINT 750,((DC(I,J),J=1,3),I=1,3)
      PRINT 751,((FEE1(I),THETA1(I)),I=1,3)
      PRINT 752,((S(K,L),K=1,3),L=1,3)                                      40
      PRINT 753,((FEE2(I),THETA2(1))I=1,3)
      PRINT 755,((RAYV(I),DEV(I)), I=1.3)
  300 PRINT 754,V(1),V(2),V(3)
      IF (NOW-1)361,320,101
  111 DO 113 I=1,3                                                          45
      G(1,I)=0.
      G(2,I)=0.
      G(3,I)=0.                                                             48
```

```
      DO 113 J=1,3                                                    49
113   DC(1,J)=0.                                                      50
      DO114 J=1,3
      DO114 I=1,3
      DO114 K=1.3
      G(1.J)=C1(I,J,K)*D(I)*D(K)+G(1,J)
      G(2,J)=C2(I,J,K)*D(I)*D(K)+G(2,J)                               55
114   G(3,J)=C3(I,J,K)*D(I)*D(K)+G(3,J)
      IF (G(1,2)*G(1,3)+G(1,2)*G(2,3)+G(1,3)*G(2,3))107,302,107
107   B(1)=-G(1,1)-G(2,2)-G(3,3)
      B1OV3=B(1)/3.0
      OB(2)=G(1,1)*G(2,2)+G(1,1)*G(3,3)+G(2,2)*G(3,3)-G(1,2)**2-G(1,3)**2 60
     1-G(2,3)**2                                                      61
      OB(3)=G(1,3)**2*G(2,2)+G(1,2)**2*G(3,3)+G(2,3)**2*G(1,1)        62
     1 -G(1,1)*G(2,2)*G(3,3)-2.0*G(1,2)*G(1,3)*G(2,3)
      ALF=B(2)-B(1)*B1OV3
      BET=2.0*B1OV3**3-B(2)*B1OV3+B(3)                                65
      BETOV2=BET/2.0
      ALFOV3=ALF/3.0
      CUAOV3=ALFOV3**3
      SQBOV2=BETOV2**2
      DEL=SQBOV2+CUAOV3                                               70
      IF(DEL)740,720,730
720   GAM=SQRTF(-ALFOV3)
      IF(BET)722,722,721
721   V(1) = -2.0*GAM-B1OV3
      V(2)=GAM-B1OV3                                                  75
      V(3)=V(2)
      GO TO 750
722   V(1)=2.0*GAM-B1OV3
      V(2)=-GAM-B1OV3
      V(3)=V(2)                                                       80
      GO TO 750
730   CUAOV3=-SQBOV2
      GO TO 720
740   QUOT=SQBOV2/CUAOV3
      ROOT=SQRTF(-QUOT)                                               85
      IF(BET)742,741,741
741   PHI=(1.5707963+ASINF(ROOT))/3.0
      GO TO 743
742   PHI=ACOSF(ROOT)/3.0
743   FACT=2.0*SQRTF(-ALFOV3)                                         90
      V(1)=FACT*COSF(PHI)-B1OV3
      V(2)=FACT*COSF(PHI+2.0943951)-B1OV3
      V(3)=FACT*COSF(PHI+4.1887902)-B1OV3
750   DO 210 I=1,3
      T(1,I)=G(2,3)*(G(1,1)-V(I))-G(1,2)*G(1,3)                       95
      T(2,I)=G(1,3)*(G(2,2)-V(I))-G(1,2)*G(2,3)
```

```
210 T(3,I)=G(1,2)*(G(3,3)-V(I))-G(1,3)*G(2,3)                    100
    DC(1,1)=1.
    DC(2,1)=1.
    DC(3,1)=1.
    DO 116 I=1,3
    DC(I,2)=T(1,I)/T(2.I)                                        105
116 DC(I,3)=T(1,I)/T(3,I)
    GO TO 108
302 IF(G(2,3))303,304,303
303 I=2
    J=3                                                         110
    K=1
    GO TO 309
304 IF(G(1,3))385,306,385
385 I=1
    J=3                                                         115
    K=2
    GO TO 309
306 IF(G(1,2))307,308,307
307 I=1
    J=2                                                         120
    K=3
309 V(K)=G(K,K)
    OV(I)=.5*(G(I,I)+G(J,J))
    1+.5*SQRTF((G(I,I)+G(J,J))**2-4.*(G(I,I)*G(J,J)-G(I,J)**2))
    OV(J)=.5*(G(I,I)+G(J,J))                                    125
    1-.5*SQRTF((G(I,I)+G(J,J))**2-4.*(G(I,I)*G(J,J)-G(I,J)**2))
    DC(K,K)=1.
    DC(I,I)=1.
    DC(I,J)=(V(I)-G(I,I))/G(I,J)
    DC(J,I)=1.                                                  130
    DC(J,J)=(V(J)-G(I,I))/G(I,J)
    GO TO 108
308 V(1)=G(1,1)
    V(2)=G(2,2)
    V(3)=G(3,3)                                                 135
    DC(1,1)=1.
    DC(2,2)=1.
    DC(3,3)=1.
108 DCNORM1=SQRTF(DC(1,1)**2+DC(1,2)**2+DC(1,3)**2)
    DCNORM2=SQRTF(DC(2,1)**2+DC(2,2)**2+DC(2,3)**2)             140
    DCNORM3=SQRTF(DC(3,1)**2+DC(3,2)**2+DC(3,3)**2)
    DO 119 I=1.3
    DC(1,I)=DC(1,I)/DCNORM1
    DC(2.I)=DC(2,I)/DCNORM2
119 DC(3,I)=DC(3,I)/DCNORM3                                     145
    DO 117 M=1,3
    S(1,M)=0.                                                   147
```

```
      S(2,M)=0.                                                      148
117   S(3,M)=0.                                                      149
      DO118 M=1,3                                                    150
      DO118 J=1,3
      DO118 K=1,3
      DO118 L=1,3
      S(1,M)=S(1,M)+C1(J,K,L)*DC(M,J)*(DC(M,K)*D(L)+D(K)*DC(M,L))
      S(2,M)=S(2,M)+C2(J,K,L)*DC(M,J)*(DC(M,K)*D(L)+D(K)*DC(M,L))     155
118   S(3,M)=S(3,M)+C3(J,K,L)*DC(M,J)*(DC(M,K)*D(L)+D(K)*DC(M,L))
      DO120 I=1,3
      SNORM(I)=SQRTF(S(1,I)**2+S(2,I)**2+S(3,I)**2)
      S(1,I)=S(1,I)/SNORM(I)
      S(2,I)=S(2,I)/SNORM(I)                                         160
120   S(3,I)=S(3,1)/SNORM(I)
      DO 121 I=1,3
121   V(I)=SQRTF(V(I)/ROW)
      DO 383 I=1,3
      THETA1(I)=ACOSF(DC(I,3))                                       165
      DIVIDE(I)=SINF(ABSF(THETA1(I)))
      THETA1(I)=THETA1(I)*57.295780
      IF(DIVIDE(I))398,399,398
399   FEE1(I)=0.
      GO TO 383                                                      170
398   DC(I,1)=DC(I,1)/DIVIDE(I)
      IF (DC(I,1)-1.)400,400,401
401   DC(I,1)=1.
400   FEE1(I)=ACOSF(DC(I,1))*57.295780
      IF (DC(I,2))825,383,383                                        175
825   FEE1(I)=360.00000-FEE1(I)
383   CONTINUE
      DO 395 K=1.3
      THETA2(K)=ACOSF(S(3,K))
      DIVIDE(K)=SINF(ABSF(THETA2(K)))                                180
      THETA2(K)=THETA2(K)*57.295780
      IF(DIVIDE(K))396,397,396
397   FEE2(K)=0.
      GO TO 395
396   S(1,K)=S(1,K)/DIVIDE(K)                                        185
      IF (S(1,K)-1.)402,402,403                                      186
403   S(1,K)=1.                                                      187
402   FEE2(K)=ACOSF(S(1,K))*57.295780
      IF(S(2,K))831,395,395
831   FEE2(K)=360.00000-FEE2(K)                                      190
395   CONTINUE
      DO 340 I=1.3
      DEV(I)=S(1.I)*D(1) +S(2,I)*D(2) +S(3,I)*D(3)
      IF (DEV(I)-1.)342,342,341
341   DEV(I)=1.                                                      195
```

```
342 RAYV(I)=V(I)/DEV(I)
340 DEV(I)=ACOSF(DEV(I))*57.295780
    GO TO 331
103 FORMAT (A8,A8,A8,A8,A8)
106 FORMAT (9F7.4)                                                    200
128 FORMAT(A8,A8,A8,A8,A8,///)
3880FORMAT (33X,15HROTATED IN THE ,2I3,17H PLANE,ABOUT THE ,I3,
    15H-AXIS//)
609 FORMAT (F10.3,F7.1,10I6)
610 FORMAT (1H1)                                                      205
7490FORMAT (F8.2,10H DEG.FROM,12,6H-AXIS,,F8.2,10H DEG.FROM,12,
    15H-AXIS)
750 FORMAT (8X,5HDVDC ,3(3(E11.4.1X).3X))
751 FORMAT (8X,5HDVDG ,3(F11.4,13X,F11.4,3X))
752 FORMAT (8X,5HPVDC ,3(3(E11.4,1X),3X))                             210
753 FORMAT (8X,5HPVDG ,3(F11.4,13X,F11.4,3X)
754 FORMAT (8X,5HPLWV ,8X,2(E13.6,6H M/SEC,19X),E13.6,6H M/SEC)
755 FORMAT (8X,5HRVDV ,3(F11.4,13X,F11.4,3X))
361 CONTINUE
    END                                                               215
```

SAMPLE DATA.

```
QUARTZ CRYSTAL                                                          1
0.8694                  0.0696 0.1743        0.1743  0.1560    .        2
      0.3999 0.1743 0.3999            0.1743                            3
      0.1743 0.5762 0.1743            0.5762                            4
      0.3999 0.1743 0.3999            0.1743                            5
0.0696                  0.8694-0.1743        -0.1743 0.1560             6
0.1743                  -0.1743 0.5762       0.5762                     7
      0.1743 0.5762 0.1743            0.5762                            8
0.1743                  -0.1743 0.5762       0.5762                     9
0.1560                  0.1560               1.0680                    10
   2650.0    1.     5    90     5    0   120    5    1    2    3    1  11
   2650.0    1.    90    90    90    0   180    5    1    3    2    1  12
   2650.0    1.    90    90    90    0   180    5    2    3    1    1  13
   2650.0  100.     1     1     1    0 36000 4500    1    2    3    2  14
POTASSIUM BROMIDE                                                      15
.3460                   .0580                       .0580             16
      .0505        .0505                                              17
             .0505                    .0505                           18
      .0505        .0505                                              19
.0580                   .3460                       .0580             20
                              .0505         .0505                     21
             .0505                    .0505                           22
                              .0505         .0505                     23
.0580                   .0580                       .3460             24
   2750.5    1.    90    90    90    0    90    5    1    2    3    0  25
```
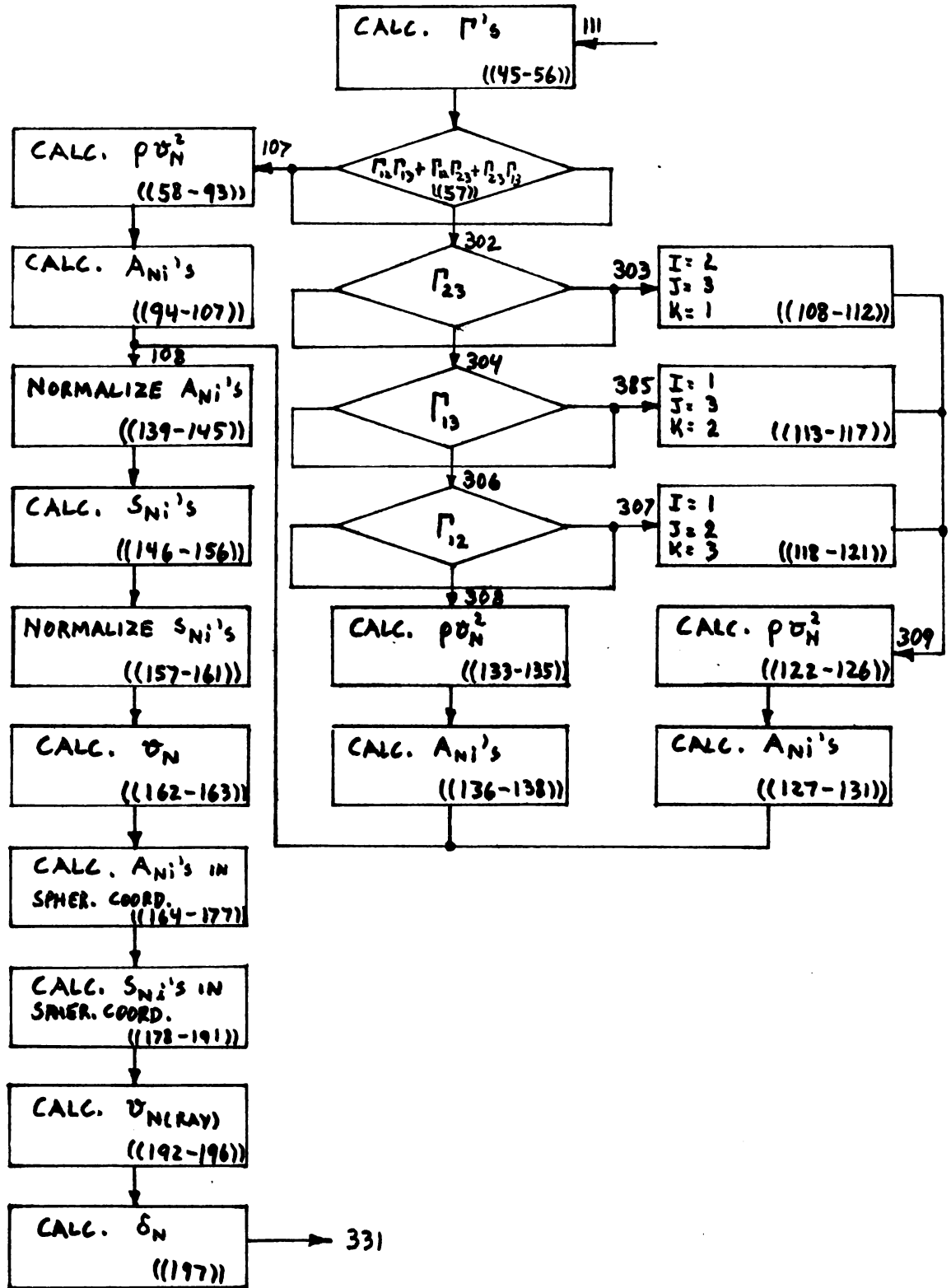
SYMBOL CROSS-REFERENCE TO COMPUTER NOTATION

$$\rho_0 \quad = \quad \text{ROW}$$

$$\rho\, v_i^2 \quad = \quad \text{V(I)} \quad ((45 - 162))$$

$$v_i \quad = \quad \text{V(I)}$$

$$c_{ijkl} \quad = \quad \text{Cl(J,K,L)}$$

$$l_i \quad = \quad \text{D(I)}$$

$$\Gamma_{ij} \quad = \quad \text{G(I,J)}$$

$$A_{Ni} \quad = \quad \text{DC(N,I)}$$

$$P_{Ni} \quad = \quad \text{S(I,N)}$$

$$\phi_{A_N} \quad = \quad \text{FEE1(N)}$$

$$\theta_{A_N} \quad = \quad \text{THETA1(N)}$$

$$\phi_{P_N} \quad = \quad \text{FEE2(N)}$$

$$\theta_{P_N} \quad = \quad \text{THETA2(N)}$$

$$v_{N(RAY)} \quad = \quad \text{RAY V(N)}$$

$$\delta_N \quad = \quad \text{DEV(N)}$$
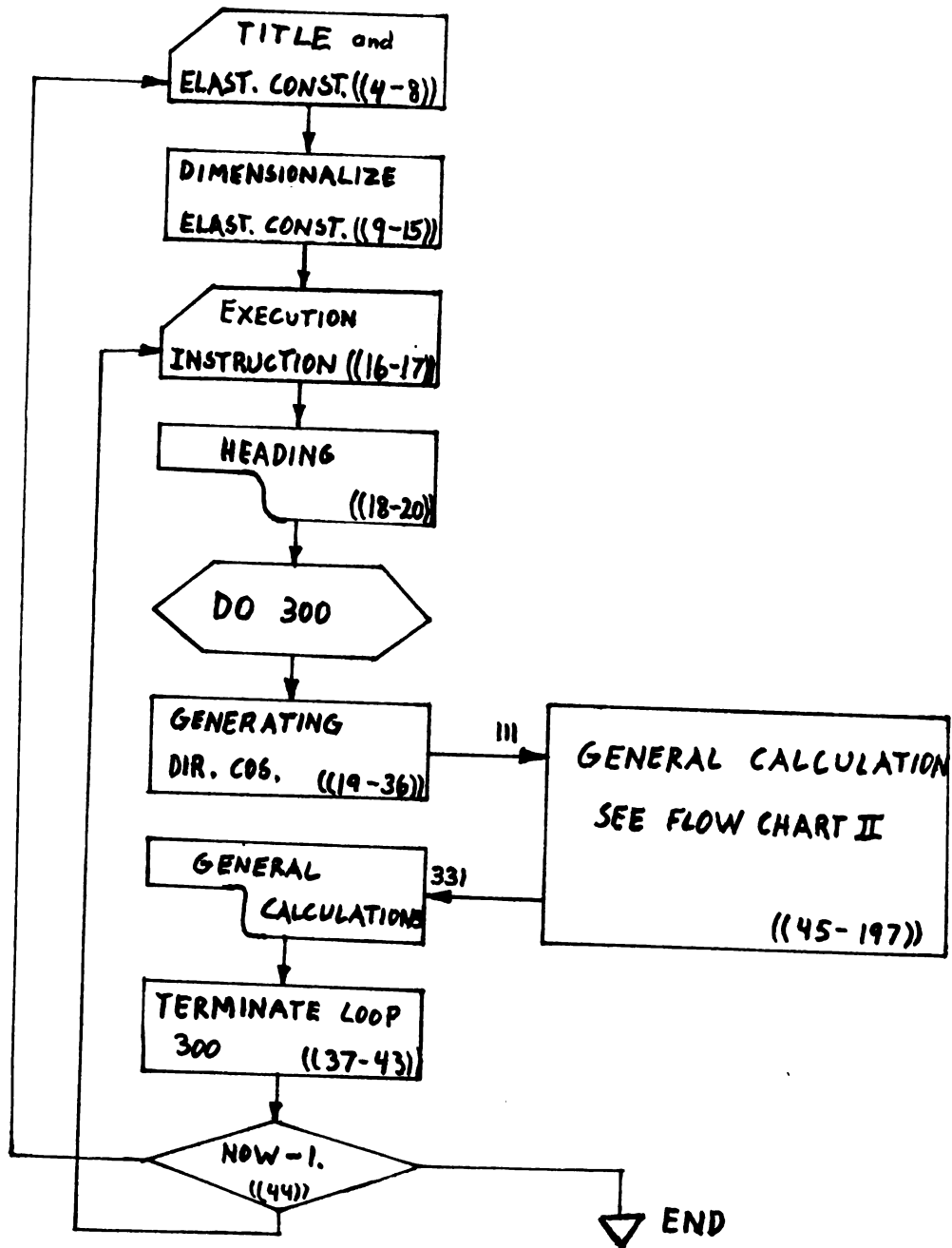
FLOW CHART I

FLOW CHART II

BIBLIOGRAPHY

1. Huygens, C., 1690, see translation, 1912, _Treatise on Light_, (translated by Silvanus P. Thompson), (London, McMillian).

2. Fresnel, A., 1827, _Oeuvres_ (Paris, Imprimerie Imperiale).

3. Christoffel, E. B., 1877, Ann. di Mat., $\underline{8}$, 193.

4. Kelvin, Lord, 1904, _Baltimore Lectures_ (Cambridge, University Press).

5. Love, A. E. H., 1927, _A Treatise on the Mathematical Theory of Elasticity_ (University Press, Cambridge, England).

6. Musgrave, M.J.P., 1954b, Proc. Roy. Soc., $\underline{226}$, 356.

7. Musgrave, M.J.P., 1956, Proc. Roy. Soc., $\underline{236}$, 352.

8. Musgrave, M.J.P., 1957b, Proc. Camb. Phil. Soc., $\underline{53}$, 897.

9. Staudte, J. H. and Cook, B. D., J. Acoust. Soc. Am., (to be published).

10. Musgrave, M.J.P., 1954a, Proc. Roy. Soc., $\underline{226}$, 339.

11. Nye, J. F., 1964, _Physical Properties of Crystals_ (Oxford Clarendon Press).

12. Farnell, G. W., 1961, Can. J. Phys., $\underline{39}$, 65.